Reinforcement of metal with liquid-exfoliated inorganic nano-platelets

Peter May, Umar Khan and Jonathan N Coleman

School of Physics, CRANN and AMBER, Trinity College Dublin, Dublin 2, Ireland

*colemaj@tcd.ie

ABSTRACT: We have prepared metal matrix composites (MMCs) of a pewter alloy filled with liquid-exfoliated Molybdenum Telluride ($MoTe_2$) nano-platelets. The combination of $MoTe_2$ and pewter was chosen due to their near-identical densities, thus reducing the scope for buoyancy-induced separation during melt mixing. The addition of nanofiller results in a doubling of the Young's modulus, Y, for a volume fraction, V_f, of <1 % $MoTe_2$, corresponding to a reinforcement of dY/dV_f =110 GPa. We find that this degree of reinforcement to be reasonably consistent with that predicted by a simplified version of Halpin-Tsai theory.

Over the last decade, the study of 2-dimensional (2D) nano-materials has become one of the most active areas of nanoscience. Since the discovery of graphene[1] and more recently, the surge of interest in inorganic 2D materials,[2-4] such nanostructures have been used to demonstrate a host of applications in areas from composites to energy storage to optoelectronics.[2-5] Particularly important will be applications which harness the impressive mechanical properties of 2D nano-materials. It is well known that graphene is the strongest, stiffest material known to man with strength and elastic modulus values of 130 and 1000 GPa respectively.[6] Indeed graphene nanosheets have been used in a number of mechanical applications particularly as a reinforcing filler in composites.[7-9] Less well known is the fact that boron nitride (BN) nanosheets display very similar mechanical properties to graphene.[10] Indeed a host of 2D nano-materials have Young's moduli which surpass 100 GPa.[11] Perhaps more importantly these materials may have strengths[11] as high as 36 GPa (estimated for layered WO_2 assuming its strength, σ_B, and modulus, Y, scale in a manner similar to MoS_2: $Y=11.7\sigma_B$)[12]. However, to the author's knowledge only three papers describe using inorganic 2D materials to mechanically reinforce any matrices; in all cases reinforcement of polymer matrices with BN nanosheets.[13-15]

In many ways this is surprising. It was recently shown that a range of layered compounds can be exfoliated by sonication in liquids to give large quantities of 2D nanosheets.[16-19] The advantage of such liquid processing is that the resultant suspensions can be used to make a range of materials and structures including composites.[3] Because of the exceptional mechanical properties of 2D materials,[11] we would expect such composites to display enhanced mechanical properties.

The vast majority of reports on nano-composites describe using nano-materials to reinforce polymer matrices.[8] Yet, many other types of composites exist; including for

example composite mixtures of two types of nanomaterial.[20-22] One particularly interesting type of nano-composite which is of great technological importance is the metal matrix composite (MMC). These composites employ filler materials to improve the thermal, electrical and mechanical properties of metals, often aluminium and magnesium. Of nano-material-reinforced MMCs, much attention has been devoted to using carbon nanotubes (CNTs) to reinforce metals.[23-36] Additionally, Boron Nitride nanotubes have been used to reinforce aluminium.[37] Only recently have reports surfaced where two dimensional filler materials have been utilised in MMCs. In each case the filler was graphene[38] or graphene oxide[9,24] while the matrix was aluminium. Impressive results were achieved with a near-doubling of tensile strength observed in one case.[9]

However, there is reason to believe that inorganic 2D materials may offer some advantages as fillers in MMCs. Several accounts from the literature highlight the presence of aggregation of CNTs either on the metal surface[30-32] or within fissures in the metal matrix[35]. Such agglomerations may arise due to large density differences between filler and matrix phases within the composite resulting in buoyancy-induced separation during mixing in the molten state.[39] This will be a particular problem when attempting to disperse low density materials such as CNTs (densities <2000 kg/m^3) in denser metals such as aluminium or titanium (2700 and 4500 kg/m^3 respectively). Layered materials, on the other hand, have a range of densities from ~2200 kg/m^3 for BN to ~9400 for WTe_2, allowing the matching of filler density to that of the matrix thus reducing the scope for demixing.

Here we demonstrate that liquid-exfoliated 2D materials, specifically $MoTe_2$ can be dispersed in a metal matrix, leading to mechanical reinforcement. In this proof of concept study, we use a low-melting point metal alloy, pewter, to facilitate melt mixing. The specific choice of 2D filler/metal combination was made such that their densities were within 5% of each other. While the dispersion was not perfect, it was reasonably good, leading to a doubling of stiffness relative to the metal itself.

The first stage in the production of the pewter/$MoTe_2$ composites studied in this work is the exfoliation of $MoTe_2$ layered crystals to give exfoliated $MoTe_2$ nano-platelets. Powdered $MoTe_2$ (www.materion.com, M-1105, Density 7700 kg/m^3, particle size <10 μm) was added to 80ml N-methylpyrrolidone (NMP) at a concentration of 15mg/ml. This mixture was sonicated overnight (15 hours) with a sonic tip (Sonics and Materials Inc, GEX600 at 25% of 600W using a flat head probe). A pulsed setting (5s on, 5s off) was used to minimise solvent heating. To maximise the concentration, the dispersion was not centrifuged. For these samples, centrifugation was not absolutely necessary as the small size of the $MoTe_2$ particles means no large unexfoliated crystallites remain after sonication. A few ml of the resulting dispersion was dropped onto a holey carbon grid (400 mesh) and analysed using a Jeol 2100 Transmission Electron Microscope (TEM) operating at 200kV. The images showed partially exfoliated nanosheets to be present in the dispersion, as shown in Fig 1A. These nanosheets were found to have an average length of $\langle L \rangle$ = 620±470 nm. For exfoliated nano-platelets such as these, it is difficult to accurately estimate the flake thickness. However, it is clear from the TEM images that while the $MoTe_2$ has been exfoliated to some degree, the platelets

still consist of a number of stacked flakes and so have thicknesses which are probably at least a few nm. This dispersion was then filtered using a 0.45 μm pore size nylon membrane to form a powder of weakly bound nano-platelets.[40]

For this work we choose a low-melting point metal to facilitate melt-mixing of the metal and nanosheets. We identified a high-grade lead-free pewter, usually used for home-casting of toy soldiers (www.princeaugust.ie, PA-2060, 94.5% Tin / 3% Zinc / 2.5% Antimony – Melting Point 230° C – Density 7346 kg/m^3), as it could be easily melted on a hot plate. An as-received 80g ingot of this metal is shown in Fig 1B.

A high $MoTe_2$ content (15wt%) masterbatch was produced by first melting 8g of pewter in a glass vial on a hot plate at 240°C. When the metal reached a molten state, the required mass of $MoTe_2$ powder was added and the mixture was stirred using a high speed rotor (a spatula blade attached to a power tool rotating at 15000 RPM) for 5 minutes. Once homogenised, the mixture was allowed to cool to form a powder. The degree of dispersion of nano-materials in metal matrices is usually controlled by a combination of the effectiveness of the mixing procedure, the degree with which the molten metal wets the nano-material surface and the density issues described above.[39] Because of the density matching achieved here, we expect the degree of dispersion of the $MoTe_2$ nano-platelets in the master batch to be limited by the crudeness of our mixing procedure as well as interfacial interactions at the pewter/$MoTe_2$ interface. Different mass fraction composites were made by adding the required amounts of masterbatch to already molten pewter in separate vials. Each sample was stirred at high speed and cooled to form a powder as before. The various composite powders were then placed onto a Kapton (melting point ~400C) sheet and heated using the hot plate. When molten once more, the samples were pressed and cooled to form thin metal sheets. These were cut into strips of width 2.25 mm and average thickness ~100μm using a die cutter.

To investigate the composition of the films, thin lamellae of both pewter-only and 1.5wt% composite films were prepared using a Zeiss Orion Focused Ion Beam Microscope (FiB). Upon examination of the surfaces using a Zeiss Ultra Scanning Electron microscope (SEM), a number of islands were observed dotted on the surface (not shown). Elemental analysis (EDX) confirmed that these islands were Zinc, with Antimony and Tin present in the background. There was no difference in grain boundary or island concentration between the pewter and the composite. In addition, SEM was also used to examine fracture surfaces of the pewter-only and 1.5wt% composite films. The fracture surface of the pewter only sample was relatively featureless, as shown in Fig 1D. However, for the composite film, clumps of aggregated platelets (1-2μm in size) were observed uniformly distributed throughout the fracture surface as seen in Fig 1E. This suggests the MoS_2 nano-platelets are not perfectly dispersed within the metal matrix. However, some regions of fracture surface were found where non-aggregated platelet-like objects could be seen protruding from the surface (fig. 1F). EDX confirmed these objects to be $MoTe_2$.

Mechanical measurements were performed on a piece of as-bought pewter, strips of pewter processed in the same way as the composites and composites of various mass

fractions using a Zwick Roell tensile tester with a 100N load cell at a strain rate of 5mm/min. For each mass fraction 5-8 strips were tested and the results averaged. Representative stress strain curves are shown in Fig 2A. The stress-strain curves for the pewter samples are similar to those reported for both Tin alloys[41] and Zinc-Antimony alloys[42]. However, processing tends to increase the tensile strength, reduce the strain at break while leaving the modulus largely unchanged. Analysis of the processed pewter stress-strain curves gave values of Young's modulus, tensile strength and strain at break of: Y=0.97±0.37 GPa, σ_B=45±11 MPa and ε_B=13±3 % respectively. It is clear from the curves in figure 2A that adding $MoTe_2$ results in a noteworthy increase in modulus coupled with a significant decrease in strain at break.

The Young's modulus is plotted as a function of $MoTe_2$ volume fraction in Fig 2B (the as-bought pewter modulus is shown for comparison). The modulus increases linearly (dY/dV_f=110±10 GPa), reaching a maximum of Y=1.93±0.6 GPa for a $MoTe_2$ content of 1vol%, before falling off at higher $MoTe_2$ contents, probably due to aggregation effects. The maximum value corresponds to a doubling in modulus relative to both as-bought and processed pewter. To the best of our knowledge this is the first report of a modulus increase for MMCs filled with 2D nano-materials.

It is worth considering whether such modulus increases are as-expected. We can analyse the data using the well-known Halpin-Tsai model for reinforcement of continuous matrices with in-plane aligned platelets. Such in-plane alignment has been observed for composites of both graphene and BN nanosheets in polymer matrices.[7,13] The Halpin-Tsai equations describe the composite modulus, Y, as a function of the filler volume fraction, V_f, the moduli of filler, Y_F, and matrix, Y_M, as well as the platelet aspect ratio, L/t. This model has been shown to describe composites of BN nanosheets in polymer matrices and some MMCs quite well.[13,43] Within this model, the composite modulus is given by[44]

$$Y = Y_M \left[\frac{1 + 2V_f \eta L/t}{1 - V_f \eta} \right] \quad (1)$$

where

$$\eta = \frac{Y_F / Y_M - 1}{Y_F / Y_M + 2L/t} \quad (2)$$

For composites where $Y_F / Y_P >> 1$, as is generally the case, the second expression can be rewritten as

$$\eta \approx \left[1 + 2\frac{L/t}{Y_F / Y_M} \right]^{-1} \quad (3)$$

By inspection, it can be seen that this expression limits the range of values for η to $0 \le \eta \le 1$. As a result, and because most nano-composites have low filler content, we can make the approximation that $V_f \eta << 1$, allowing us to combine equations 1 and 3 in a simplified form:

$$Y \approx Y_M + \frac{Y_F V_f}{\left[\frac{Y_F / Y_M}{2L/t} + 1\right]} \quad (4)$$

This equation is useful because it predicts the rate of increase of modulus with volume fraction, dY / dV_f, to depend on properties of matrix and filler in a simple way:

$$\frac{dY}{dV_f} \approx \frac{Y_F}{\left[\frac{Y_F / Y_M}{2L/t} + 1\right]} \quad (5)$$

From figure 2B, we know that dY / dV_f =110±10 GPa and Y_M≈1 GPa. Thus, equation 5 defines a relationship between Y_F and L/t which must be fulfilled for the Halpin-Tsai equations to accurately describe these composites. As far as we are aware there are no direct experimental measurements of the Young's modulus of $MoTe_2$ nano-platelets. However, a number of measurements have shown the stiffness of MoS_2 nanosheets to be in the range 270-330 GPa[12,45]. In addition, theoretical calculations of the in-plane stiffness of a range of layered crystals show that (when corrected for differences in monolayer thickness)[46] the modulus of $MoTe_2$ is approximately 60% of that of MoS_2.[11] This allows us to estimate the stiffness of $MoTe_2$ nano-platelets to be in the range 160-200 GPa. Then using equation 5 with the measured values of dY / dV_f and Y_M shows that, if the Halpin-Tsai model is applicable here, the mean nano-platelet aspect ratio should be in the range $100 \le L/t \le 160$. Given that the mean flake length was measured to be 620±470 nm and the thickness of an $MoTe_2$ monolayer is 0.7 nm,[46] this means the nano-platelets would have to consist of <15 stacked monolayers on average for the Halpin-Tsai equations to be accurate. This seems reasonable. Solvent exfoliated graphene tends to consist of flakes with thickness in the range 1-5 monolayers.[47] It is clear from the TEM images such as that in figure 1A that these $MoTe_2$ nano-platelets are relatively poorly exfoliated compared to graphene. However, it is certainly possible that they consist of <15 monolayers. We note that if the true mean thickness of the nano-platelets in this work is greater than 15 monolayers, then this implies that the mean aspect ratio is <100. This means that, for the Halpin-Tsai model to accurately describe the data, the modulus of the $MoTe_2$ would have to be greater than 200 GPa. On the other hand, if the flakes turned out to be thicker than 15 monolayers, it could also mean the Halpin-Tsai does not apply here, resulting in larger than expected composite stiffness.

The tensile strength does not increase significantly compared to the processed pewter as $MoTe_2$ is added (figure 2C). However, as the $MoTe_2$ content is increased beyond 1% the strength falls off, reaching ~10 MPa for 6% $MoTe_2$. However, we note that the strength of all samples with $MoTe_2$ content below 5% had strength greater than the as-bought pewter.

Previous studies have observed strength increases at relatively low loading level followed by a falloff at higher filler content for MMCs filled with both carbon nanotubes[25,26,32] and graphene[24]. A strength decrease, often at higher loading levels is commonly observed for nanomaterial-filled polymer composites.[7,13,48] Such behaviour has been attributed to filler aggregation.[49] As such, degradation of strength with $MoTe_2$ content is to be expected given the platelet aggregation observed in Fig 1E. The strain at break also decreases relatively uniformly with increased levels of $MoTe_2$. This behaviour has been observed for several other MMCs[9,24,25,28,30,32,34] and indeed polymer nano-composite materials [7,13,48,50-55].

In conclusion, we have demonstrated a method to prepare composites of exfoliated $MoTe_2$ nano-platelets in a metal matrix. Use of a low melting point matrix such as pewter simplifies the process of melt mixing while matching filler and matrix densities reduced the propensity for buoyancy driven de-mixing. While such processing results in sub-optimal dispersion of the nano-platelets, some well-dispersed $MoTe_2$ nanosheets were observed. We found the Young's modulus of a 1% $MoTe_2$ composite to be double that of the pewter itself. Such an increase agrees reasonably well with the predictions of theory. However, both strength and strain at break fell with increasing MoTe2 content, possibly due to aggregation effects.

We acknowledge the European Research Council for financial support via the grant SEMANTICS.

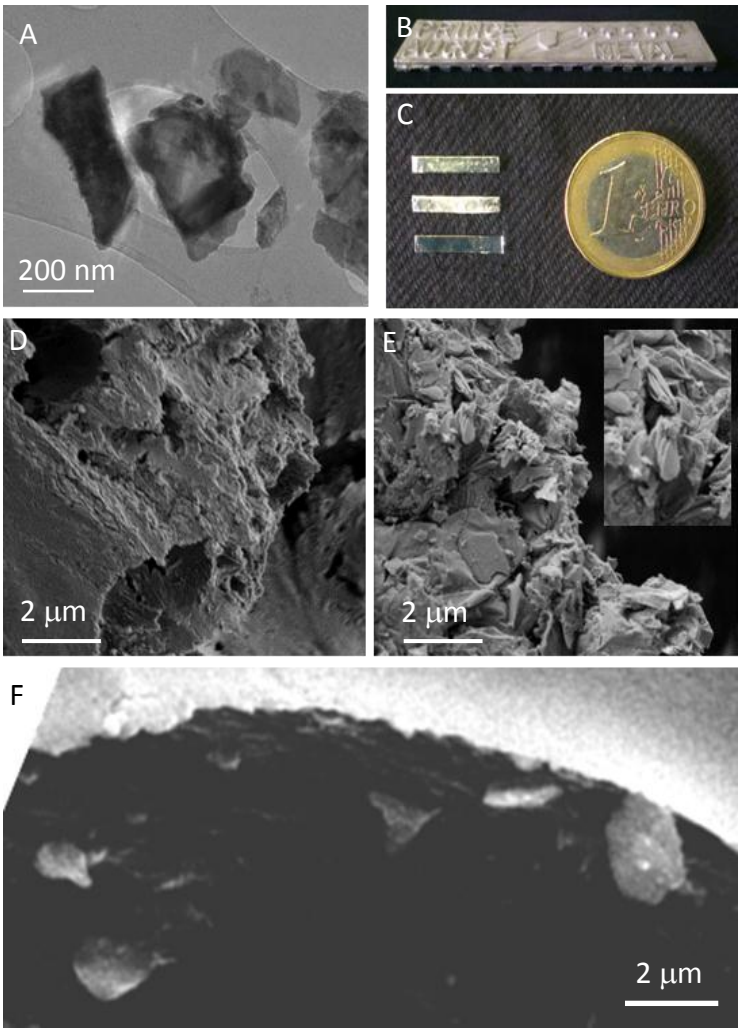

Figure 1: A) TEM images of $MoTe_2$/NMP dispersion with many multilayer nanosheets present. B) Photo of an as-received pewter ingot. C) Pewter-only (top) and composite strips used for mechanical testing. D) SEM image of pewter fracture surface. E) SEM image of a 1.5wt% composite fracture surface. F) SEM image of the fracture surface of a 1.5wt% composite film with protruding nano-platelets visible.

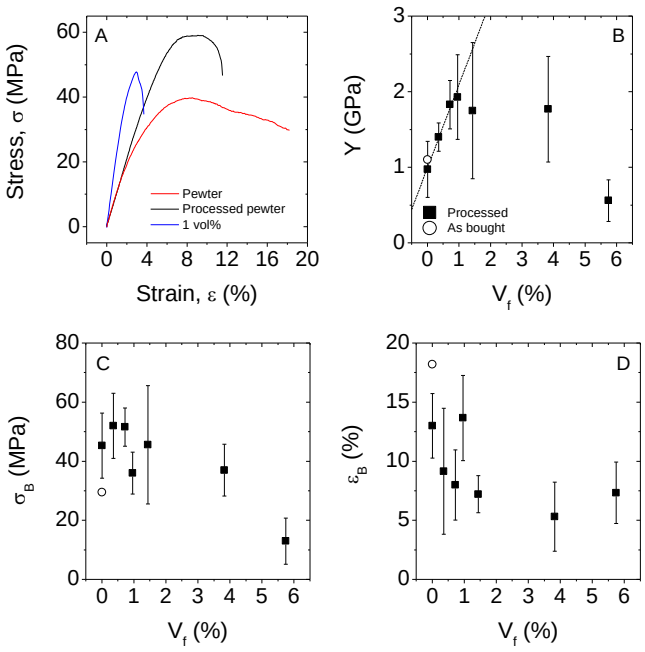

Figure 2: A) Representative stress-strain curves for a piece of as-bought pewter, a pewter-only film processed in the same manner as the composites and a composite film (1vol%). B-D) Plots of B) modulus, C) ultimate tensile strength and D) strain at break versus filler volume fraction for the processed pewter and composite films. For comparison the properties of as-bought pewter are also shown. The dashed line in B represents a slope of 125 GPa.

References

1 A. K. Geim, Science **324**, 1530 (2009).

2 M. Chhowalla, H. S. Shin, G. Eda, L. J. Li, K. P. Loh, and H. Zhang, Nat. Chem. **5**, 263 (2013).

3 V. Nicolosi, M. Chhowalla, M.G. Kanatzidis, M.S. Strano, and J.N. Coleman, Science **340**, 1226419 (2013).

4 Q. H. Wang, K. Kalantar-Zadeh, A. Kis, J. N. Coleman, and M. S. Strano, Nature Nanotechnology **7**, 699 (2012).

5 K. S. Novoselov, V. I. Fal'ko, L. Colombo, P. R. Gellert, M. G. Schwab, and K. Kim, Nature **490**, 192 (2012).

6 C. Lee, X. D. Wei, J. W. Kysar, and J. Hone, Science **321**, 385 (2008).

7 P. May, U. Khan, A. O'Neill, and J. N. Coleman, Journal of Materials Chemistry **22**, 1278 (2012).

8 T. Kuilla, S. Bhadra, D. H. Yao, N. H. Kim, S. Bose, and J. H. Lee, Progress in Polymer Science **35**, 1350 (2010).

9 J. Wang, Z. Li, G. Fan, H. Pan, Z. Chen, and D. Zhang, Scripta Materialia **66**, 594 (2012).

10 L. Duclaux, B. Nysten, J. P. Issi, and A. W. Moore, Physical Review B **46**, 3362 (1992).

11 C. Ataca, H. Sahin, and S. Ciraci, Journal of Physical Chemistry C **116**, 8983 (2012).

12 S. Bertolazzi, J. Brivio, and A. Kis, ACS Nano **5**, 9703 (2011).

13 U. Khan, P. May, A. O'Neill, A. P. Bell, E. Boussac, A. Martin, J. Semple, and J. N. Coleman, Nanoscale **5**, 581 (2013).

14 Y. Wang, Z. X. Shi, and J. Yin, Journal of Materials Chemistry **21**, 11371 (2011).

[15] C. Y. Zhi, Y. Bando, C. C. Tang, H. Kuwahara, and D. Golberg, Advanced Materials **21**, 2889 (2009).

[16] J. N. Coleman, M. Lotya, A. O'Neill, S. D. Bergin, P. J. King, U. Khan, K. Young, A. Gaucher, S. De, R. J. Smith, I. V. Shvets, S. K. Arora, G. Stanton, H. Y. Kim, K. Lee, G. T. Kim, G. S. Duesberg, T. Hallam, J. J. Boland, J. J. Wang, J. F. Donegan, J. C. Grunlan, G. Moriarty, A. Shmeliov, R. J. Nicholls, J. M. Perkins, E. M. Grieveson, K. Theuwissen, D. W. McComb, P. D. Nellist, and V. Nicolosi, Science **331**, 568 (2011).

[17] G. Cunningham, M. Lotya, C.S. Cucinotta, S. Sanvito, S.D. Bergin, R. Menzel, M.S.P. Shaffer, and J.N. Coleman, Acs Nano **6**, 3468 (2012).

[18] A. O'Neill, U. Khan, and J. N. Coleman, Chem. Mat. **24**, 2414 (2012).

[19] R. J. Smith, P. J. King, M. Lotya, C. Wirtz, U. Khan, S. De, A. O'Neill, G. S. Duesberg, J. C. Grunlan, G. Moriarty, J. Chen, J. Z. Wang, A. I. Minett, V. Nicolosi, and J. N. Coleman, Advanced Materials **23**, 3944 (2011).

[20] G. Cunningham, M. Lotya, N. McEvoy, G. S. Duesberg, P. van der Schoot, and J. N. Coleman, Nanoscale **4**, 6260 (2012).

[21] P.J. King, U. Khan, M. Lotya, S. De, and J. N. Coleman, ACS Nano **4**, 4238 (2010).

[22] V. C. Tung, L. M. Chen, M. J. Allen, J. K. Wassei, K. Nelson, R. B. Kaner, and Y. Yang, Nano Letters **9**, 1949 (2009).

[23] S. R. Bakshi, D. Lahiri, and A. Agarwal, International Materials Reviews **55**, 41 (2010).

[24] S. F. Bartolucci, J. Paras, M.A. Rafiee, J. Rafiee, S. Lee, D. Kapoor, and N. Koratkar, Materials Science and Engineering: A **528**, 7933 (2011).

[25] C. F. Deng, D. Z. Wang, X. X. Zhang, and A. B. Li, Materials Science and Engineering: A **444**, 138 (2007).

[26] A. M. K. Esawi, K. Morsi, A. Sayed, A. Abdel Gawad, and P. Borah, Materials Science and Engineering: A **508**, 167 (2009).

[27] A. M. K. Esawi, K. Morsi, A. Sayed, M. Taher, and S. Lanka, Composites Science and Technology **70**, 2237 (2010).

[28] L. Jiang, Z. Li, G. Fan, L. Cao, and D. Zhang, Carbon **50**, 1993 (2012).

[29] L. Jiang, Z. Li, G. Fan, L. Cao, and D. Zhang, Scripta Materialia **66**, 331 (2012).

[30] H. Kwon, M. Estili, K. Takagi, T. Miyazaki, and A. Kawasaki, Carbon **47**, 570 (2009).

[31] J-Z. Liao, M-J. Tan, and I. Sridhar, Materials & Design **31**, S96 (2010).

[32] Z. Y. Liu, B. L. Xiao, W. G. Wang, and Z. Y. Ma, Carbon **50**, 1843 (2012).

[33] R. Pérez-Bustamante, C. D. Gómez-Esparza, I. Estrada-Guel, M. Miki-Yoshida, L. Licea-Jiménez, S. A. Pérez-García, and R. Martínez-Sánchez, Materials Science and Engineering: A **502**, 159 (2009).

[34] X. Yang, E. Liu, C. Shi, C. He, J. Li, N. Zhao, and K. Kondoh, Journal of Alloys and Compounds **563**, 216 (2013).

[35] D. K. Lim, T. Shibayanagi, and A. P. Gerlich, Materials Science and Engineering: A **507**, 194 (2009).

[36] C. S. Goh, J. Wei, L. C. Lee, and M. Gupta, Materials Science and Engineering: A **423**, 153 (2006).

[37] M. Yamaguchi, A. Pakdel, C. Y. Zhi, Y. Bando, D. M. Tang, K. Faerstein, D. Shtansky, and D. Golberg, Nanoscale Res. Lett. **8** (2013).

[38] L-Y. Chen, H. Konishi, A. Fehrenbacher, C. Ma, J-Q. Xu, H. Choi, H-F. Xu, F. E. Pfefferkorn, and X-C. Li, Scripta Materialia **67**, 29 (2012).

[39] T. Noguchi, A. Magario, S. Fukazawa, S. Shimizu, J. Beppu, and M. Seki, Materials Transactions **45**, 602 (2004).

[40] U. Khan, H. Porwal, A. O'Neill, K. Nawaz, P. May, and J.N. Coleman, Langmuir **27**, 9077 (2011).

[41] T. Rameshkumar, I. Rajendran, and A. D. Latha, Tribology in Industry **32** (2010).

[42] F. M. Azizan, H. Purwanto, and M.Y. Mustafa, International Journal of Engineering & Technology **12**, 78 (2012).

[43] S. R. Bakshi and A. Agarwal, Carbon **49**, 533 (2011).

[44] R. J. Young, I. A. Kinloch, L. Gong, and K. S. Novoselov, Composites Science and Technology **72**, 1459 (2012).

[45] A. Castellanos-Gomez, M. Poot, G. A. Steele, H. S. J. van der Zant, N. Agraït, and G. Rubio-Bollinger, Advanced Materials **24**, 772 (2012).
[46] J. A. Wilson and A. D. Yoffe, Advances in Physics **18**, 193 (1969).
[47] U. Khan, A. O'Neill, M. Lotya, S. De, and J. N. Coleman, Small **6**, 864 (2010).
[48] H. Hu and G. Chen, Polymer Composites **31**, 1770 (2010).
[49] J. N. Coleman, U. Khan, W. J. Blau, and Y. K. Gun'ko, Carbon **44**, 1624 (2006).
[50] L. Jiang, X-P. Shen, J-L. Wu, and K-C. Shen, Journal of Applied Polymer Science, n/a (2010).
[51] J. Liang, Y. Huang, L. Zhang, Y. Wang, Y. Ma, T. Guo, and Y. Chen, Advanced Functional Materials **19**, 2297 (2009).
[52] K. Nawaz, U. Khan, N. Ul-Haq, P. May, A. O'Neill, and J. N. Coleman, Carbon **50**, 4489 (2012).
[53] K. W. Putz, O. C. Compton, M. J. Palmeri, S-B. T. Nguyen, and L. C. Brinson, Advanced Functional Materials **20**, 3322 (2010).
[54] X. Yang, L. Li, S. Shang, and X-M. Tao, Polymer **51**, 3431 (2010).
[55] Xin Zhao, Qinghua Zhang, Dajun Chen, and Ping Lu, Macromolecules **43**, 2357 (2010).